Richtmyer-Meshkov and Rayleigh-Taylor instabilities at ablation front of direct-drive laser fusion targets

A. Marocchino[1], S. Atzeni[2], A. Schiavi[2]

[1] *Dipartimento di Energetica, Università di Roma "La Sapienza", Italy*

[2] *Dipartimento di Energetica, Università di Roma "La Sapienza" and CNISM, Italy*

Introduction

Ignition target design in inertial confinement fusion (ICF) relies on accurate control of the asymmetry growth due to hydrodynamic instabilities such as the Rayleigh-Taylor instability (RTI) and the Richtmyer-Meshkov instability (RMI) [1, 2]. In this contribution we focus on the RMI developing at the ablation front (af-RMI) [3, 4] of laser irradiated targets, with the goal of studying the evolution of perturbations as a function of laser intensity I and perturbation wavelength λ.

In the classical RMI (i.e. the instability occurring when a shock crosses a corrugated interface separating two different materials) asymptotically perturbations grow linearly in time [5]. When the instability occurs at an ablation front, instead, perturbations with sufficiently short wavelength oscillate and are rapidly damped [3, 4]. They exhibit a Bessel-J like behaviour. Longer perturbations still grow.

Damping is essentially due to thermal conduction and is effective on perturbations with mode number $k = 2\pi/\lambda$ such that $kD_c > 1$, where D_c is the distance spanning between critical density for laser propagation and the ablation front, i.e. the thickness of the layer where the laser-deposited energy is transported to the ablation front by thermal conduction [3, 4]. This distance depends on target material, laser wavelength λ_{laser} and intensity I. Here we consider D_2 or DT targets and uv laser light, with $\lambda_{laser} = 0.35\ \mu$m.

Numerical aspects

We have conducted a numerical study via high resolution 2D lagrangian simulations, using the DUED code [6], with a two-temperature model (radiation is indeed found to play a minor role in the considered targets). An appropriate equation-of-state is used. Thermal conduction is described by a standard flux-limited model, with flux-limiting coeffiicient $f = 0.06$ (sharp cut-off). Laser light irradiates normally the target, and is absorbed by inverse Bremsstrahlung. We initialise single wavelength perturbations via surface roughness, or density inhomogeneity in a specific target layer.

We used simulation meshes adequate to resolve the details of the ablation layer, where the

density scalelength can be extremely small, especially at relatively modest laser irradiances. For instance, in simulations with $I = 4 \times 10^{12}$ W/cm^2, where $L_m \leq 0.1$ μm, we used an initial mesh spacing as small as 3×10^{-3} μm (in the direction of the laser) in the region of the target facing the laser.

Care was also taken to filter numerical hour-glass mesh oscillations without affecting the behaviour of physical instabilities.

Thick targets: af-RTI

We have first considered thick targets, where such effects as feed-through and feed-out, shock reflection and target acceleration do not occur, and the RMI behaviour is easily evidenced. The perturbation seed is surface corrugation. Simulations referring to a D_2 target and intensity $I = 4 \times 10^{14}$ clearly show (see Fig. 1) that ablation front perturbations with wavelength $\lambda \leq 40$ μm oscillate with short period (≤ 1 ns) and are rapidly damped. Perturbations with $\lambda = 50$–100 μm decay slowly, while those with longer λ oscillate with amplitudes clearly exceeding the initial value (see the curve for $\lambda = 200$ μm in Fig. 1).

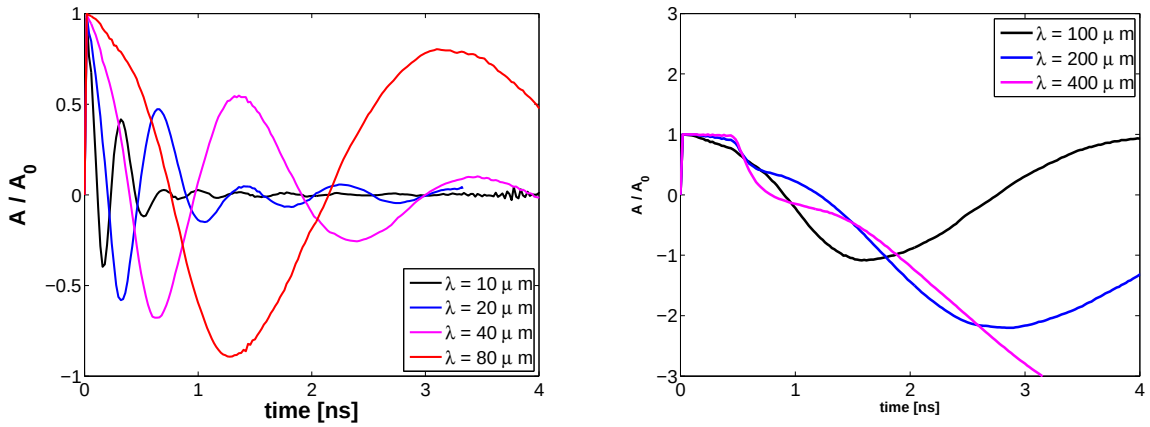

Figure 1: Evolution of ablation front perturbations with different wavelengths λ, for thick D_2 targets, irradiated by flat pulse with intensity $I = 4 \times 10^{14}$ W/cm^2. the initial surface roughness perturbation has an amplitude of $A_0 = 10^{-5}$ cm. Left frame: wavelengths $\lambda = 10, 20, 40, 80$ μm ; right frame: wavelengths $\lambda = 100, 200, 400$ μm .

When the laser intensity is decreased (and then the conduction layer shrinks), the wavelength threshold for damping decreases as well. Figure 2, referring to the previous set-up, but intensity $I = 4 \times 10^{12}$ W/cm^2, indeed shows that in this case perturbations with $\lambda = 10$ μm and 20 μm oscillate with amplitude much larger than the initial one.

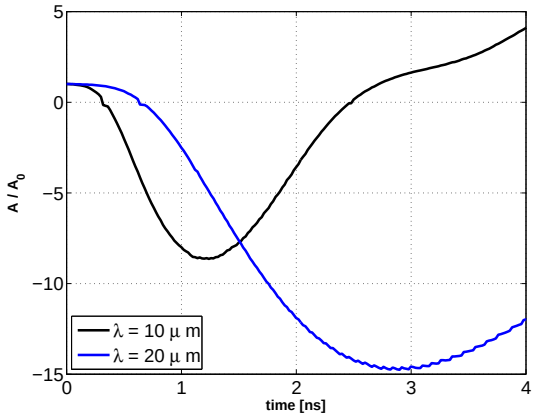

Figure 2: Evolution of af-RTI. Same as Fig. 1, but for laser intensity $I = 4 \times 10^{12}$ W/cm^2.

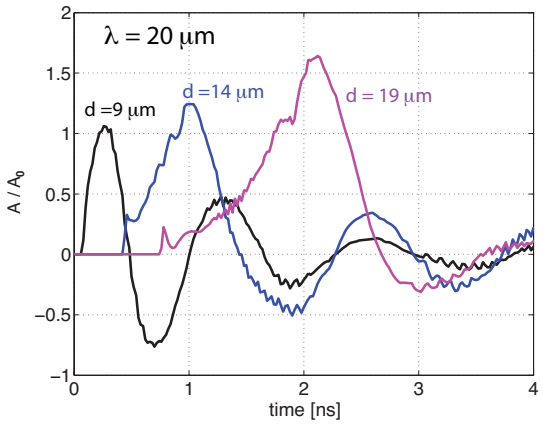

Figure 3: Same as Fig. 1, but for perturbations with $\lambda = 20$ μm, seeded as density inhomogeneity in a 5 μm thick layer at depths d from the target surface, from the laser side.

It is to be noticed that when we consider a target with perfectly flat surfaces, but with a thin inhomogeneous layer, we still observe damped oscillation after shock transit, as shown in Fig. 3.

Thin targets: af-RMI and af-RTI

Typical ICF direct-drive targets are thin shells, and are driven by time-shaped laser pulses, usually consisting of a relatively long foot, followed by a ramp and a high-intenity plateau. The foot drives a first shock, which causes af-RMI. When the whole shell is set to motion and is accelerated by the main pulse, RTI occurs.

To get insight into this sequence of processes we have considered a planar *DT* target with parameters analogous to those of the (spherical) baseline target considered in the HiPER project. For the target see Ref. [7], for an updated pulse shape see Ref. [8] and [9]. The foil we simulate has thickness of 211 μm, initial density of 0.25 g/cm^3 and temperature of 20 K. The foil is first crossed by shocks and start accelerating after about 7 ns from the beginning of the laser (foot)-pulse.

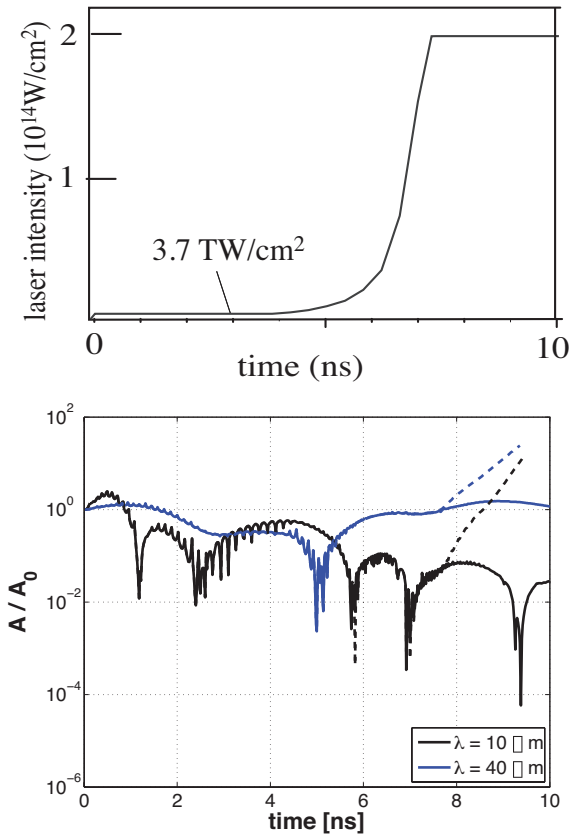

Figure 4: DT targets driven by a time-shaped pulse. Upper frame: laser intensity vs time; lower frame: ablation front perturbations with $\lambda = 10, 40$ μm. Solid curves: thick target; dashed curves: thin target.

Figure 4 shows the evolution of ablation front perturbations with $\lambda = 10$ μm and 40 μm. Af-RMI oscillations are observed at $t < 7$ ns, and RTI exponential growth for $t > 7$ ns. The af-RMI thus contributes to seeding af-RTI. In this context, it should be observed that shorter wavelengths (roughly, $\lambda \leq 20\,\mu$m in the present case, corresponding to spherical modes with mode number $l \geq 300$) are smoothed by RMI. This is an encouraging result for direct-drive ICF. We also notice that adiabat-shaping techniques [10] can also be used to reduce af-RMI and af-RTI growth as well.

This work was partially supported by the Italian MIUR project PRIN 20072KW45J, which funds AM position. SA and AS gratefully acknowledge the support of the HiPER project and Preparatory Phase Funding Agencies (EC, MSMT and STFC) in undertaking this work. AS positions at CNISM is funded by STFC.

References

[1] J. D. Lindl, Inertial Confinement Fusion, Springer, New York (1998).

[2] S. Atzeni J. and J. Meyer-ter-Vehn, The Physics of Inertial Fusion, Oxford University Press (2004).

[3] V. N. Goncharov, Phys. Rev. Lett., **82**, 2091 (1999).

[4] V. N. Goncharov et al., Phys. Plasmas, **13**, 012702 (2006).

[5] R. D. Richtmyer, Commun. Pure Appl. Math. **13**, 297 (1960).

[6] S. Atzeni et al., Computer Phys. Commun. **169**, 153 (2005).

[7] S. Atzeni, A. Schiavi and C. Bellei, Phys. Plasmas **14**, 052702 (2007).

[8] L. Hallo et al., Plasma Phys. Controll. Fusion **51**, 014001 (2009).

[9] S. Atzeni et al., Nucl. Fusion **49**, 055008 (2009)

[10] K. Anderson and R. Betti, Phys. Plasmas **11**, 5 (2004).